

## Some Results on Multiplicity Correlations in Catastrophic Destruction of $^{12}\text{C}$ -AgBr Collisions at 4.5 AGeV

Praveen Prakash Shukla<sup>1</sup>, H. Khushnood<sup>2</sup> and M. Saleem Khan<sup>1</sup>

<sup>1</sup>Department of Applied Physics, MJPR University, Bareilly-243001

<sup>2</sup>University Polytechnic, Jamia Millia Islamia, New Delhi-110025

**Abstract:** An attempt has been made to investigate some interesting features of  $^{12}\text{C}$ -AgBr collisions at 4.5 AGeV. It is found that probability of catastrophic destruction of heavy emulsion nuclei increases with the increasing mass of nuclei and the angular distribution of charged shower particles depends on the mass of projectile. Furthermore several multiplicity correlations have also been investigated.

**Key words:** Catastrophic destruction, angular distribution, charged shower particles, multiplicity distribution, multiplicity correlations.

### I. Introduction:

The Study of peripheral collisions of relativistic heavy ion interactions is attracting a great deal of attention during the recent years [1-8]. It may be due to the fact that the study of totally disintegrated events produced in heavy ion collisions, in which almost the whole projectile takes part in the reactions [1-8]. The probability of total disintegration of Ag and Br nuclei of nuclear emulsion is quite small, leading to low statistics of the experimental data. Nevertheless, the study of catastrophic destructions is extremely important because during such collisions, the nuclear matter might be compressed to several times, its normal density and consequently several interesting phenomena are expected to occur. The study of catastrophic destructions of relativistic nuclei can throw some light on the probability of investigating the effects of multi-nucleon interactions, collective properties of nuclear matter, production of shock waves in nuclear matter and its possible transitions to the quark gluon phase. Furthermore some characteristics of the catastrophic destructions are more critical to the choice of the collision model. Thus, the experimental data on catastrophic destructions may also be used to refine the existing models, put forward for explaining the dynamics of multi-particle production in relativistic heavy ion interactions.

### II. Experimental technique:

In the present work, an emulsion stack of several pellicles of NIFKI-BR2 type is used. The size of each Pellicle is  $18.7 \times 9.7 \times 0.06 \text{ cm}^3$ . The stack was exposed by 4.5 AGeV carbon nuclei at Dubana Synchrotron, Russia. A random sample of 681 events was picked up by using along the track doubly scanning method. All charged secondaries emitted or produced in an interaction are classified in accordance with their ionization or normalized grain density ( $g^*$ ), range (L) and velocity ( $\beta$ ) into the following categories:

**2.1 Shower tracks ( $N_s$ ):** These are freshly created charged particles with  $g^*$  less than 1.4. These particles have  $\beta > 0.7$ . They are mostly fast pions with a small mixture of Kaons and released protons from the projectile which have undergone an interaction. For the case of proton, kinetic energy ( $E_p$ ) should be less than 400 MeV.

**2.2 Grey tracks ( $N_g$ ):** Particles with range  $L > 3 \text{ mm}$  and  $1.4 < g^* < 6.0$  are defined as greys. They have  $\beta$  in the range of  $0.3 < \beta < 0.7$ . These are generally knocked out protons of targets with kinetic energy in between 30 - 400 MeV, and traces of deuterons, tritons and slow mesons.

**2.3 Black tracks ( $N_b$ ):** Particles having  $L < 3 \text{ mm}$  from interaction vertex from and  $g^* > 6.0$ . This corresponds to  $\beta < 0.3$  and protons of kinetic energy less than 30 MeV. Most of these are produced due to evaporation of residual target nucleus.

The number of heavily ( $N_h$ ) ionizing charged particles ( $N_h$ ) are part of the target nucleus is equal to the sum of black and grey fragments ( $N_h = N_b + N_g$ ).

All the experimental details may be found in our earlier publication [2].

### III. Experimental Results and Discussions:

#### 3.1 Dependence of probability of catastrophic destruction of AgBr on projectile mass:

It is reported that the events having at least 28 heavily ionizing tracks i.e.  $N_h \geq 28$  may be classified as events of total disintegrations of Ag and Br nuclei [1-3]. The reason for including disintegrations with  $N_h \geq 28$  in various analysis might be due to the fact that these events correspond to a total charge closed to the average charge of Ag and Br [ $Z=41$ ] and hence they cause a very high degree of breakup of the target nucleus. Thus for studying various characteristics of secondary particles produced in catastrophic destruction of  $^{12}\text{C}$ -nucleus collisions at 4.5 AGeV, we have carried out a search for the events with  $N_h \geq 28$ . An important characteristic of the catastrophic destruction of heavy emulsion nuclei induced by very fast projectile, is the probability ( $A_p$ ) which is the ratio of the number of events having  $N_h \geq 28$  and the total number of disintegrations involving Ag and Br nuclei. The probabilities of total break up of AgBr nuclei in heavy ion interactions at 4.5 A GeV along with other projectiles at the same energy are listed in the table 1. It may be seen in the table 1, that the probability of catastrophic destruction of heavy emulsion nuclei increases with the increasing mass of projectile.

**Table 1:** Probabilities of total disintegration of AgBr nuclei in 4.5 A GeV/c nucleus-nucleus collisions

Projectile	S (GeV)	Probability (%)	Reference
Deuteron	5.10	2.60±0.50	8
$\alpha$ -particle	9.42	6.80±0.90	8
Carbon	24.09	11.85±1.32	Present work
Carbon	24.09	11.70±1.00	10

The probability  $W(A_p)$  of the total disintegration of Ag and Br nuclei caused by 4.5 AGeV carbon nuclei, as a function of projectile mass is plotted in fig.1. It may be of interest to point out that the solid line shown in fig.1 can be represented by the following relation:

$$W(A_p) = \alpha A^\beta$$

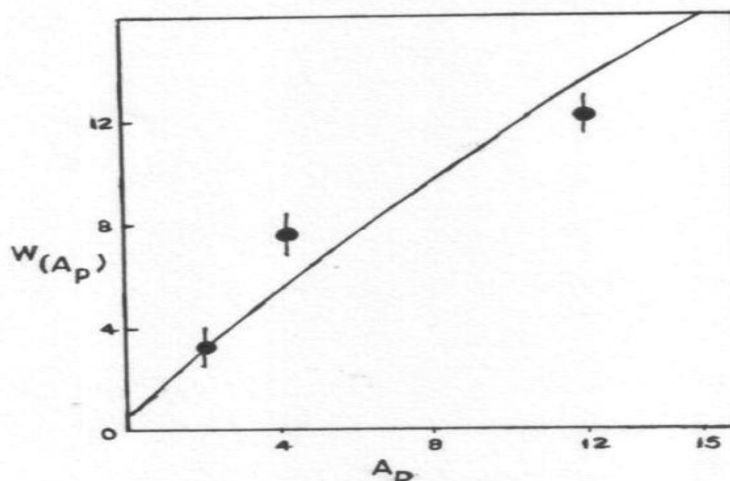


Fig.1 Variation of the probability of central collisions with the mass of the projectile

The best fitting value of parameters  $\alpha$  and  $\beta$  are  $(1.82 \pm 0.18)$  and  $(0.80 \pm 0.24)$  respectively. Values of these parameters obtained by Tauseef Ahmad et al [9] are  $1.99 \pm 0.27$  and  $0.82 \pm 0.05$  respectively.

#### 3.2 Multiplicity correlations:

Several workers have attempted to study the multiplicity correlations among various charged secondaries produced in nucleus-nucleus collisions [11-14] for events having  $N_h \geq 0$ . However a little attention has been paid for studying the multiplicity correlations of these secondary charged particles in catastrophic destruction of Ag and Br nuclei caused by the projectile [10]. Multiplicity correlations of the type  $\langle N_i(N_j) \rangle$ , where  $N_i, N_j = N_b, N_g, N_s$  and  $i \neq j$  have been studied for the total disintegration events produced in  $^{12}\text{C}$ -nucleus interaction, and are presented in the following sections.

##### 3.2.1 Variations of $\langle N_g \rangle$ , $\langle N_h \rangle$ and $\langle N_s \rangle$ with $N_b$ :

The variations of  $\langle N_g \rangle$ ,  $\langle N_h \rangle$  and  $\langle N_s \rangle$  as a function of  $N_b$  are shown in fig.2. It is obvious from the figure that the value of  $\langle N_g \rangle$  and  $\langle N_h \rangle$  grows with the increase of  $N_b$  while the value of  $\langle N_s \rangle$  is found to decrease

with increasing value of  $N_b$ . However it has been reported by other workers that the shower and grey particles have similar multiplicity dependence on  $N_b$ [10]. Thus our results do not agree with those reported in ref.[10]. The least square fits of the experimental points have also been indicated in the fig.2. The following eq. (1-3) represents these fits quite well:

$$\langle N_g \rangle = (-0.42 \pm 0.11) N_b + (25.70 \pm 1.71) \quad (1)$$

$$\langle N_h \rangle = (0.82 \pm 0.02) N_b + (23.06 \pm 1.91) \quad (2)$$

$$\langle N_s \rangle = (0.46 \pm 0.25) N_b + (8.32 \pm 2.85) \quad (3)$$

### 3.2.2 Variations of $\langle N_b \rangle$ , $\langle N_h \rangle$ and $\langle N_s \rangle$ with $N_g$ :

The dependence of parameters  $\langle N_b \rangle$ ,  $\langle N_h \rangle$  and  $\langle N_s \rangle$  on  $N_g$  are exhibited in fig.3. It is noticed by this figure that  $\langle N_h \rangle$  increases almost linearly with  $N_g$ , whilst, both  $\langle N_b \rangle$  and  $\langle N_s \rangle$  decreases with increasing value of  $N_g$ . This result is in marked disagreement with those obtained in [10]. The experimental data may be fitted with the following eq. (4-6) obtained by the method of least squares:

$$\langle N_b \rangle = (-0.76 \pm 0.10) N_g + (27.19 \pm 2.08) \quad (4)$$

$$\langle N_h \rangle = (0.60 \pm 0.18) N_g + (20.75 \pm 3.65) \quad (5)$$

$$\langle N_s \rangle = (-0.40 \pm 0.09) N_g + (21.88 \pm 1.93) \quad (6)$$

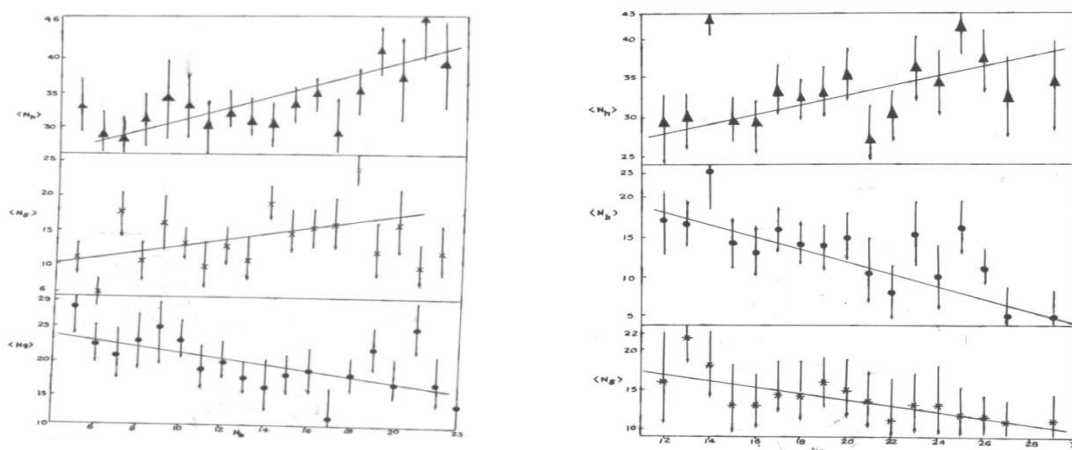


Fig.2 variations of  $\langle N_g \rangle$ ,  $\langle N_h \rangle$  and  $\langle N_s \rangle$  as a function of  $N_b$  with  $N_g$  Fig.3 Variations of  $\langle N_b \rangle$ ,  $\langle N_h \rangle$  and  $\langle N_s \rangle$  as a function of  $N_b$  with  $N_g$

### 3.2.3 Variations of $\langle N_b \rangle$ , $\langle N_g \rangle$ and $\langle N_s \rangle$ on $N_h$ :

Fig. 4 shows the variations of  $\langle N_b \rangle$ ,  $\langle N_g \rangle$  and  $\langle N_s \rangle$  on  $N_h$ . On the same fig. we have plotted solid lines correspond to the following relationship (7-9), fitted by the method of least squares:

$$\langle N_b \rangle = (0.60 \pm 0.11) N_h + (-6.47 \pm 3.97) \quad (7)$$

$$\langle N_g \rangle = (0.36 \pm 0.12) N_h + (8.10 \pm 4.42) \quad (8)$$

$$\langle N_s \rangle = (0.19 \pm 0.15) N_h + (20.59 \pm 5.28) \quad (9)$$

It is observed that values of  $\langle N_b \rangle$ ,  $\langle N_g \rangle$  increases linearly with the increase of  $N_h$  (with decreasing impact parameter). Furthermore, the parameter  $\langle N_s \rangle$  is found to decrease with an increase in  $N_h$ .

### 3.2.4 Variations of $\langle N_b \rangle$ , $\langle N_g \rangle$ , $\langle N_h \rangle$ and $\langle N_s \rangle$ as a function of $N_c$ :

In order to investigate the dependence of parameters  $\langle N_b \rangle$ ,  $\langle N_g \rangle$ ,  $\langle N_h \rangle$  and  $\langle N_s \rangle$  on the compound multiplicity, we have plotted the experimental data in fig. 5. It is clearly evident from this figure that the values of  $\langle N_g \rangle$ ,  $\langle N_h \rangle$  and  $\langle N_s \rangle$  grows rapidly with  $N_c$ . However, the value of  $\langle N_b \rangle$ , is observed to decrease with increasing value of  $N_c$ . The following eq. (10-13), obtained by the method of least squares, are found to fit with the experimental data quite satisfactorily:

$$\langle N_b \rangle = (-0.12 \pm 0.10) N_c + (16.68 \pm 3.66) \quad (10)$$

$$\langle N_g \rangle = (0.37 \pm 0.06) N_c + (7.32 \pm 1.82) \quad (11)$$

$$\langle N_h \rangle = (-0.42 \pm 0.09) N_c + (19.03 \pm 3.11) \quad (12)$$

$$\langle N_s \rangle = (0.74 \pm 0.06) N_c + (-10.40 \pm 2.12) \quad (13)$$

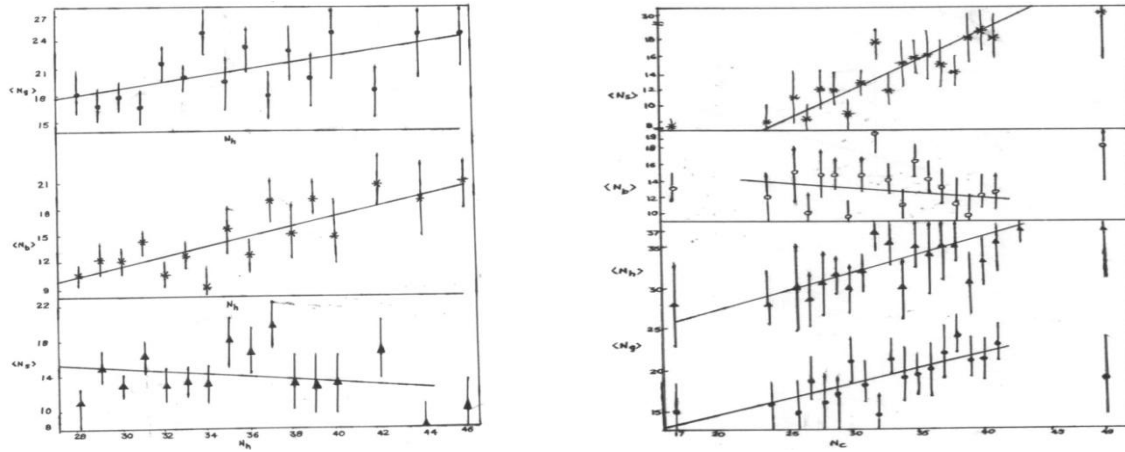


Fig.4 Dependence of  $\langle N_b \rangle$ ,  $\langle N_g \rangle$  Fig.5 Variations of  $\langle N_b \rangle$ ,  $\langle N_g \rangle$ ,  $\langle N_h \rangle$  and  $\langle N_s \rangle$  on  $N_b$  and  $\langle N_s \rangle$  on  $N_c$

### 3.2.5 Dependence of $\langle N_c \rangle$ with $N_b, N_g, N_h$ and $N_s$ :

In fig.6, the variations of  $\langle N_c \rangle$  are displayed as a function of  $N_b, N_g, N_h$  and  $N_s$ . It may be seen in the fig.6 that the value of  $\langle N_c \rangle$  is found to increase linearly with the increase in the values of  $N_b, N_g, N_h$  and  $N_s$ . The following relations (14-17), obtained by the method of least squares, are found to fit with the experimental points quite well.

$$\langle N_c \rangle = (0.36 \pm 0.20)N_b + (28.43 \pm 2.95) \quad (14)$$

$$\langle N_c \rangle = (0.78 \pm 0.10)N_g + (16.97 \pm 2.10) \quad (15)$$

$$\langle N_c \rangle = (1.30 \pm 0.17)N_h + (-7.40 \pm 5.31) \quad (16)$$

$$\langle N_c \rangle = (0.80 \pm 0.07)N_s + (23.12 \pm 1.16) \quad (17)$$

### 3.3 Dependence of $\eta$ on the projectile mass:

The angular distribution of charged shower particles produced in totally disintegrated nuclei at 4.5 A GeV has been analyzed in terms of pseudorapidity variable,  $\eta [= -\ln \tan(\theta/2)]$ , where  $\theta$  is the emission angle of a shower particle with respect to the projectile. The  $\eta$ -distributions of charged shower particles produced in central collision for carbon and silicon nuclei 4.5 A GeV is exhibited in the fig.7. It may be mentioned that the values of  $\eta$  for totally disintegrated events at 4.5 A GeV, Si-nucleus events have been taken from ref. [9]. It is observed here that  $\eta$ -distributions become wider with increasing projectile mass. Furthermore, the maxima of  $\eta$ -spectra tend to shift towards higher values of  $\eta$  with increasing projectile mass. This result is in nice agreement with the findings of Tauseef Ahmad et al [9].

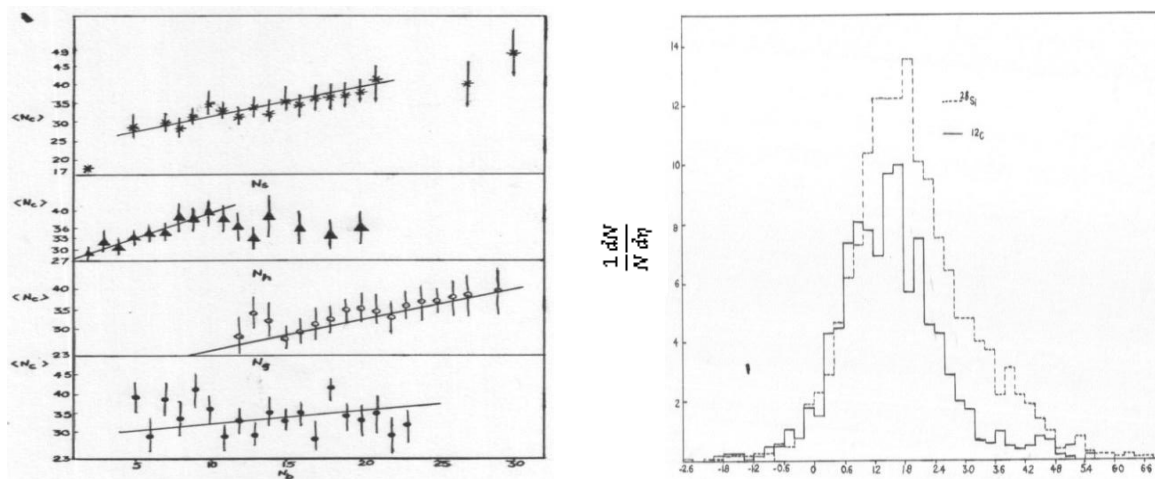


Fig.6 Dependence of  $\langle N_c \rangle$  with  $N_b, N_g, N_h$  and  $N_s$  Fig.7  $\eta$ -distribution of charged shower particles produced in central collisions at 4.5 A GeV

#### IV. Conclusions:

On the basis of the study of the totally disintegrated events of Ag and Br nuclei caused by 4.5 A GeV per nucleon carbon projectile, we draw some important conclusions which may be summarized as follows:

- (i) The probability of catastrophic destruction of Ag and Br emulsion nuclei increases with the mass of target. This result may be explained by the fact that the inelastic cross-section does not depend on the energy of the projectile, but it increases with the projectile mass.
- (ii) The average multiplicity of  $\langle N_g \rangle$  and  $\langle N_s \rangle$  increases rapidly, while  $\langle N_b \rangle$  decreases with the mass of the projectile. This result may be explained on the basis of fire ball model.
- (iii) The charged particles multiplicity correlations in the central collisions are almost similar to those obtained in all  $^{12}\text{C}$ -nucleus interactions, except that the value of the parameters  $a_{ij} \leq 0$  have been found only for the correlations  $\langle N_g \rangle - N_b$ ,  $\langle N_b \rangle - N_g$ ,  $\langle N_s \rangle - N_g$ ,  $\langle N_g \rangle - N_s$ ,  $\langle N_b \rangle - N_c$ , and  $\langle N_h \rangle - N_c$ , for the totally disintegrated events at 4.5 A GeV.
- (iv) The angular distribution of charged shower particles depends on the mass of projectile.

#### References:

- [1]. M.El-Nadi et al:Z.Phys.A310,301(1983).
- [2]. H.Khushnood et al: Can.J.Phys.64, 320(1986).
- [3]. Tauseef Ahmad et al:Can.J.Phys.67,519(1989).
- [4]. Sh. Sarfaraz Ali and H.Khushnood: Euro Phys Lett.65, 773(2004).
- [5]. Mahmoud Mohery Cand.J.Phy90 (12)1267, +1278, 2012.
- [6]. D.H.Zhang et al: Chinese Phys15 (11)2564- 2570(2006).
- [7]. M.Saleem Khan, et al Proc.DAE Int. Sym. On Nuclear Phys Vol.58 (2013).
- [8]. T. Ahmad, A study of pion-nucleus interactions in terms of compound particles, ISRN High Energy Physics, 2014 (2014).
- [9]. TauseefAhmad,MustafaAbdulslam Nasr and M.Irfan, Phys. Rev.C 47(1993).
- [10]. M. QasimRaza Khan, Ph.D. Thesis,AMU,Aligarh 1988.
- [11]. H. Khushnood, M.Saleem Khan, A.R. Ansari and Q.N. Usmani, DAE Symposium on nuclear Physics, Calicut (1993).
- [12]. A.Abdeslam:Phys.G:Nucl.Part,Phys.28,375(2002).
- [13]. M.SaleemKhan, PraveenPrakashShukla and H.Khushnood:Proc.DAE Symposium on Nuclear Physics,59(2014).
- [14]. V. G. Bogdanov et al: Sor.J.Nucl.Phys.38, 909(1983).
- [15]. A.El.Naghy et al: NuovoCim.A, 107A, 279(1994).